THE JOURNAL OF BIOLOGICAL CHEMISTRY VOL. 289, NO. 22, pp. 15666–15679, May 30, 2014

Heat-induced Irreversible Denaturation of the Camelid Single Domain VHH Antibody Is Governed by Chemical Modifications

Received for publication, November 12, 2013, and in revised form, March 29, 2014 Published, JBC Papers in Press, April 16, 2014, DOI 10.1074/jbc.M113.534222

Yoko Akazawa-Ogawa[‡], Mizuki Takashima[‡], Young-Ho Lee[§], Takahisa Ikegami[§], Yuji Goto[§], Koichi Uegaki[‡1], and Yoshihisa Hagihara[‡2]

From the [‡]National Institute of Advanced Industrial Science and Technology (AIST) , 1-8-31 Midorigaoka, Ikeda, Osaka 563-8577, Japan and [§]Institute for Protein Research, Osaka University, Yamadaoka 3-2, Suita, Osaka 565-0871, Japan

Background: The mechanism of heat-induced irreversible denaturation of a single domain VHH camelid antibody remains unclear.
Results: The denaturation of VHH did not depend on the number of refolding/unfolding reactions or protein concentration. Mutations replacing Asn increased the heat tolerance of VHH.
Conclusion: Chemical modifications are suggested to be a dominant factor for irreversible denaturation of VHH.
Significance: Our findings enable further improvements for heat tolerance of VHH.

The variable domain of camelid heavy chain antibody (VHH) is highly heat-resistant and is therefore ideal for many applications. Although understanding the process of heat-induced irreversible denaturation is essential to improve the efficacy of VHH, its inactivation mechanism remains unclear. Here, we showed that chemical modifications predominantly governed the irreversible denaturation of VHH at high temperatures. After heat treatment, the activity of VHH was dependent only on the incubation time at 90 °C and was insensitive to the number of heating (90 °C)-cooling (20 °C) cycles, indicating a negligible role for folding/unfolding intermediates on permanent denaturation. The residual activity was independent of concentration; therefore, VHH lost its activity in a unimolecular manner, not by aggregation. A VHH mutant lacking Asn, which is susceptible to chemical modifications, had significantly higher heat resistance than did the wild-type protein, indicating the importance of chemical modifications to VHH denaturation.

Increasing the robustness of antibodies against heat-induced irreversible denaturation is important for the application of antibodies as drugs, diagnostic reagents, and biosensors (1, 2). The variable domain of camelid heavy chain antibody (VHH)[3] is a single domain antibody that originates from a natural mammalian antibody (3, 4). VHH is active after incubation at high temperatures (>80 °C) and is significantly more heat-resistant than conventional antibodies (5–10). Thus, VHH is recognized as an ideal antibody for many applications. A mechanistic understanding of heat-induced irreversible denaturation will help improve VHH heat resistance and the efficacy of VHH in industrial applications; however, no information is available on the irreversible denaturation of this fragment.

Heat-induced irreversible denaturation, defined as a permanent inactivation of protein function caused by exposure to high temperature, has been considered to mainly originate from four factors: aggregation of folding intermediates, aggregation of the unfolded state, chemical modifications, and generation of misfolded monomers (11). Although each factor has been extensively studied, no study has precisely discriminated the effects of these factors on the heat-induced denaturation of antibodies. Folding intermediates often present exposed hydrophobic residues; thus, they are vulnerable to nonspecific aggregation (12–16). Moreover, many proteins aggregate at high temperatures (17, 18). Chemical modifications of amino acids are also frequently observed when a protein is heated at a high temperature (19–25). In addition, the heating process induces the formation of misfolded monomers (26), which are formed through noncovalent aberrant interactions. A precise evaluation of these factors would enable us to better understand the mechanisms of VHH heat-induced irreversible denaturation.

In this study, we first evaluated the effects of heat treatment on the refolding and/or unfolding process by measuring the residual activity of VHH using surface plasmon resonance (SPR) after two types of heat treatments. In these experiments, the samples were subjected either to repetitive 90 and 20 °C incubations or to continuous incubation at a high temperature. The remaining factors controlling denaturation, *i.e.* aggregation, misfolding, and chemical modifications of amino acids, were assessed by a series of experiments examining various parameters, including incubation temperature and protein concentration. Mutations increasing heat tolerance were then exploited. In addition, changes in biophysical properties during the VHH denaturation process were analyzed by matrix-assisted laser desorption ionization time-of-flight (MALDI-TOF) mass spectrometry, circular dichroism (CD) spectrometry,

[1] To whom correspondence may be addressed. Tel.: 81-727-51-9461; Fax: 81-727-8370; E-mail: k-uegaki@aist.go.jp.
[2] To whom correspondence may be addressed. Tel.: 81-727-51-8989; Fax: 81-727-9517; E-mail: hagihara-kappael@aist.go.jp.
[3] The abbreviations used are: VHH, variable domain of camelid heavy chain antibody; Fab, antigen-binding fragment; scFv, single chain variable fragment; hCG, human chorionic gonadotropin; SPR, surface plasmon resonance; T_m, midpoint temperature of thermal unfolding; DSC, differential scanning microcalorimetry; Gdn-HCl, guanidine hydrochloride; HBS-EP, 10 mM HEPES (pH 7.4), 150 mM NaCl, 3 mM EDTA, and 0.005% surfactant P20.

and differential scanning microcalorimetry (DSC). Finally, we identified the critical determinant of VHH heat-induced denaturation.

EXPERIMENTAL PROCEDURES

Materials—Mouse anti-human chorionic gonadotropin (hCG) IgG clone 207 was purchased from Wako Pure Chemical Industries, Ltd. (Osaka, Japan), and IgG clone 28A4 and IgG clone 77F12 were from HyTest, Ltd. (Turku, Finland). Single chain variable fragment (scFv) clone 1001.1E5.E8 was from Randox Life Sciences Co. (Antrim, UK). hCG and *Bacillus cereus* β-lactamase (penicillinase) were obtained from Sigma-Aldrich.

Preparation of VHH and Fab Fragments—Wild-type anti-hCG (VHH-H14) and anti-β-lactamase (cAbBCII10) VHH synthetic genes were designed using the published peptide sequences (27–31). Construction of the expression vectors containing anti-hCG wild-type and mutant VHHs with an artificial disulfide bond was described previously (32, 33). Asn residues at positions 52, 74, and 84 of anti-hCG VHH were replaced with Ser, Ser, and Thr, respectively, by PCR-based site-directed mutagenesis. The resulting mutant, N52S/N74S/N84T, was cloned into pAED4 (34). Wild-type and mutant VHHs were expressed in *Escherichia coli* strain BL21(DE3) pLysS (Stratagene, La Jolla, CA) using Lennox LB medium. Anti-hCG VHHs were accumulated in inclusion bodies, and anti-β-lactamase VHH was expressed in soluble form. Inclusion bodies from 1.6 liters of culture were suspended with 3 ml of 10 mM Tris-HCl (pH 8.5) and 100 μl of 1 M dithiothreitol and solubilized by addition of 3 g of solid guanidine hydrochloride (Gdn-HCl). These samples were then purified on Superdex 75 columns (GE Healthcare) pre-equilibrated with 6 M urea in 10 mM Tris-HCl (pH 8.5) and subjected to overnight air oxidation at 4 °C. A 1/10 volume of 1 M sodium acetate (pH 4.7) was added to the samples, and samples were then dialyzed against 10 mM sodium acetate (pH 4.7). A Resource S cation-exchange column (GE Healthcare) equilibrated with 10 mM sodium acetate (pH 4.7) was used to purify crude VHHs. When anti-hCG wild-type VHH was expressed in synthetic medium, it could be recovered from soluble and insoluble fractions of cell extracts. The histidine-tagged constructs of anti-hCG and anti-β-lactamase VHHs in which the sequence of Ala-Gly-Gly-His-His-His-His-His-His was appended to the C terminus of the sequence were prepared, and proteins were expressed in synthetic or LB medium. The soluble fraction and the insoluble fraction, dissolved in 6 M Gdn-HCl, were subjected to 5-ml HiTrap Chelating HP or HisTrap HP columns (GE Healthcare) and eluted by a gradient of imidazole and NaCl in 20 mM Tris-HCl buffer (pH 8.5). Anti-β-lactamase VHH was incubated in 6 M Gdn-HCl and 10 mM Tris-HCl (pH 8.5) overnight at room temperature to oxidize the disulfide bond and extensively dialyzed against 10 mM Tris-HCl (pH 8.5). Formation of the disulfide bond was confirmed by Ellman's reagent (35). A MALDI-TOF mass spectrometer (Microflex AI, Bruker Daltonics Inc., Billerica, MA) was then used to confirm that the molecular weight of the purified proteins was identical to the expected values calculated from their amino acid sequences (with an error of ±0.025%) with an added N-terminal Met residue. Three antigen-binding fragments (Fabs), Fab clone 207, Fab clone 28A4, and Fab clone 77F12, were prepared from IgG clone 207, IgG clone 28A4, and IgG clone 77F12, respectively, using the Pierce Fab preparation kit (Thermo Fisher Scientific Inc., Rockford, IL). Briefly, 0.5 mg of IgG was treated with 0.5 ml of immobilized papain (250 μg/ml of settled resin) for 18 h at 37 °C, and the Fc fragment was removed using immobilized protein A. The concentration of VHH in the stock solution was determined by measuring the absorbance at 280 nm (36) using a UV-2500PC spectrophotometer (Shimadzu Corp., Kyoto, Japan). The concentration of Fab was determined by the absorption at 280 nm using an extinction coefficient of 1.4 for 1 mg/ml.

Iterative Heat-induced Heating-Cooling Cycles and Continuous Incubation—Treatment of the antibodies with iterative heating-cooling cycles was carried out using GeneAmp PCR System 9700 and 2700 thermal cyclers (Invitrogen), a PTC-0150 MiniCycler (Bio-Rad), and TaKaRa PCR Thermal Cycler SP and Dice Standard (Takara Bio Inc., Shiga, Japan). Samples in 10 mM HEPES (pH 7.4), 150 mM NaCl, 3 mM EDTA, and 0.005% surfactant P20 (HBS-EP) were divided into 160-μl aliquots placed in 0.2-ml microtubes. Ramp speeds of thermal cyclers ranged from 1.2 to 1.9 °C/s for heating and from 0.8 to 1.3 °C/s for cooling. To equilibrate the structural change of proteins, the samples were incubated for 5 min after increase or decrease of temperature. In typical heating-cooling cycles, samples were heated for 5 min at 90 °C and then incubated for 5 min at 20 °C. Continuous heating experiments were also performed under the same conditions without multiple heating-cooling cycles (see Fig. 1*A*).

Measurement of the Antigen Binding Activities of VHH and Other Antibodies—β-Lactamase was purified by HisTrap HP (GE Healthcare) equilibrated by 10 mM Tris-HCl (pH 7) and 1 mM $ZnCl_2$ (37). Antigen hCG (0.05 mg/ml) and β-lactamase (0.025 mg/ml) were coupled to a CM5 sensor chip (GE Healthcare) in 10 mM sodium acetate buffer (pH 4.7) by amine coupling according to the manufacturer's instructions. Analysis was performed on a Biacore 2000 instrument (GE Healthcare) in HBS-EP buffer at 20 °C followed by regeneration with 10 mM glycine (pH 2.0) and 0.5 M NaCl. The interaction between VHH and hCG in this study could not be approximated by the simple Langmuir model (33). Therefore, we estimated the residual activity using standard curves for VHH, scFv, three Fabs, and three IgGs (see Fig. 1, *B–E*). For the generation of standard curves, the SPRs of four to five untreated intact samples with known protein concentrations between 0.1 and 2 μg/ml were measured. The protein concentrations were plotted against SPR values at 350 s at which the antibody association section was almost finished. Using these standard curves, the SPR values of heat-treated samples at 350 s were converted into residual active antibody fractions. Estimated residual activity of anti-hCG VHH using the SPR values of controls and samples at 150, 200, 250, 300, and 350 s were not significantly deviated and were almost identical to each other within the errors (Fig. 1*F*). When the sample concentration was higher than 2 μg/ml, it was diluted with HBS-EP buffer before SPR measurement. Typically, the residual activity of VHH was measured at a protein concentration of 1.3 μg/ml, corresponding to 100 nM. For each measurement, the data were at least duplicated using a multiple

channel flow cell, and data were averaged. Errors were calculated as standard deviations.

Analytical Gel Permeation Chromatography and SDS-PAGE—Wild-type VHH samples (10 μM) with or without heat treatment were first filtered by spin column with a 0.45-μm PVDF membrane (Ultrafree-MC, EMD Millipore Corp., Billerica, MA). The samples (200 μl; 10 μM) were analyzed using Superose 6 10/300 GL (GE Healthcare) equilibrated with HBS-EP buffer at room temperature. In addition, 10 μl of the same samples was subjected to SDS-PAGE on 10–20% gels (Oriental Instruments Ltd., Tokyo, Japan) with or without dithiothreitol as a reducing reagent.

MALDI-TOF Mass Spectra of Heat-treated VHH and the N52S/N74S/N84T Mutant—Wild-type VHH and the N52S/N74S/N84T mutant (5 μM) were subjected to 40 cycles of heating (90 °C)-cooling (20 °C) or to a continuous 1,600-min incubation at 90 °C in HBS-EP buffer. The samples were mixed volume to volume with 10 mg/ml synaptic acid (Nacalai Tesque, Kyoto, Japan) in 80% acetonitrile with 0.1% 2,2,2-trifluoroacetic acid. MALDI-TOF mass spectra were obtained using a Microflex AI instrument.

Measurement of Equilibrium Thermal Unfolding of VHH and Mutants—Circular dichroism spectra were measured using a J-820 spectropolarimeter (Jasco) and a 1-mm cell in 10 mM HEPES (pH 7.4), 150 mM NaCl, and 0.005% surfactant P20, which is HBS-EP buffer without EDTA, at a protein concentration of 25 μM unless otherwise noted. Thermal unfolding of VHH and mutants with or without heat treatment was monitored as the change in ellipticity at 235 nm under the above conditions. After the first thermal unfolding, the consecutive second thermal unfolding curve was almost identical to that of the first run for both wild-type and mutant VHH with and without heating-cooling cycles, confirming the reversibility of VHH from the thermally unfolded state. DSC measurements of VHH were made using a VP-DSC microcalorimeter (MicroCal, Northampton, MA) in HBS-EP buffer. For both CD and DSC measurements, the heating rate was 1 °C/min.

Treatment of Heat-treated VHH with Denaturant—To unfold heat-treated VHH, 400 mg of solid Gdn-HCl was added to 300 μl of wild-type VHH (40 μM) in HBS-EP buffer, resulting in a final concentration of denaturant of ~6 M. The samples were then dialyzed against 10 mM HEPES (pH 7.4), 150 mM NaCl, and 0.005% surfactant P20. The VHH concentrations of dialyzed samples were estimated using absorbance at 280 nm and comparison with that of samples with known VHH concentrations. CD spectra of dialyzed samples were measured at a protein concentration of 14 μM at 37 °C without dilution or concentration. The fraction of residual activity was evaluated against the activity of Gdn-HCl-treated VHH without heat treatment to minimize potential experimental error caused by an additional denaturant-induced unfolding and refolding step.

RESULTS

Irreversible Denaturation of VHH Was Induced by Iterative Heat-induced Heating-Cooling Cycles and Continuous Treatment at a High Temperature—The impact of folding/unfolding intermediates on the irreversible denaturation of VHH was determined. The residual antigen binding activity after iterative heating (90 °C for 5 min)-cooling (20 °C for 5 min) cycles or continuous incubation at 90 °C was measured using SPR (Figs. 1 and 2*A*). VHH-H14, the VHH clone used in these experiments, recognizes hCG and has been widely used as a model of VHH molecules (5, 6, 10, 27, 32, 33, 38–40). Its midpoint temperature of thermal unfolding (T_m) is 65 °C, and other VHHs reported are considered to be unfolded at 90 °C (7, 31). Thus, we chose 90 °C as the heating temperature. The proteins were treated for 5 min at 90 °C in heating-cooling cycles; the number of cycles multiplied by 5 min corresponded to the continuous incubation time. If the folding/unfolding intermediates are important for denaturation, the residual activity after a certain number of cycles should be lower than the activity after continuous incubation for the same total heating time. However, the denaturation curves as a function of the number of cycles and the continuous incubation time were almost identical (Fig. 2*A*). Our results suggested that VHH denaturation did not depend on aggregation and/or misfolding of VHH folding/unfolding intermediates in our experimental conditions.

Next, VHH samples were treated with various heating temperatures ranging from 40 to 90 °C (Fig. 2*B*). In these experiments, 80 cycles and 400 min of continuous heating were selected in which ~20% of the antigen binding activity remained when heating temperature was 90 °C (Fig. 2*A*). Heat-induced denaturation of VHH was observed at 70 °C and above, but no significant denaturation was observed at 60 or 65 °C. At these temperatures, which are close to the T_m (65 °C), ~20–50% of the molecules were unfolded (32, 33) (see also Fig. 8*B*). Because an equilibrium reaction between the native and unfolded states often occurred at 60 and 65 °C, this finding also supported the minor role of the folding/unfolding intermediates in VHH denaturation. More than 90% of the molecules were already unfolded at 70 °C, but increasing the temperature led to a decrease in VHH residual activity, suggesting that the thermal load of the unfolded state may cause denaturation, whereas higher temperatures may accelerate it. Indeed, at a low temperature of ~37 °C, VHH remained fully active for 1 year in solution (Fig. 2*B*, *inset*).

The VHH protein used in the above experiments was recovered from inclusion bodies and refolded; thus, it may have different properties, such as refolding ability and tendency to aggregate, than VHH protein recovered from soluble fractions. However, soluble VHH expressed in *E. coli* presented an identical denaturation curve against continuous heating compared with that of the VHH protein obtained from inclusion bodies (Fig. 3*A*), confirming that the preparation of VHH did not substantially affect our experimental result.

For comparison, anti-β-lactamase VHH was also subjected to heat-induced denaturation by the heating-cooling cycles and continuous incubation (Fig. 3*B*). Similar to anti-hCG VHH, denaturation curves of anti-β-lactamase VHH induced by heating-cooling cycles and continuous incubation were almost identical. It should be noted that residual activities after a heat treatment less than 25 min or five cycles were ~10% higher than that of non-treated sample, and this phenomena would make further analysis ambiguous. Thus, anti-hCG VHH was chosen as a representative of VHH for further experiments.

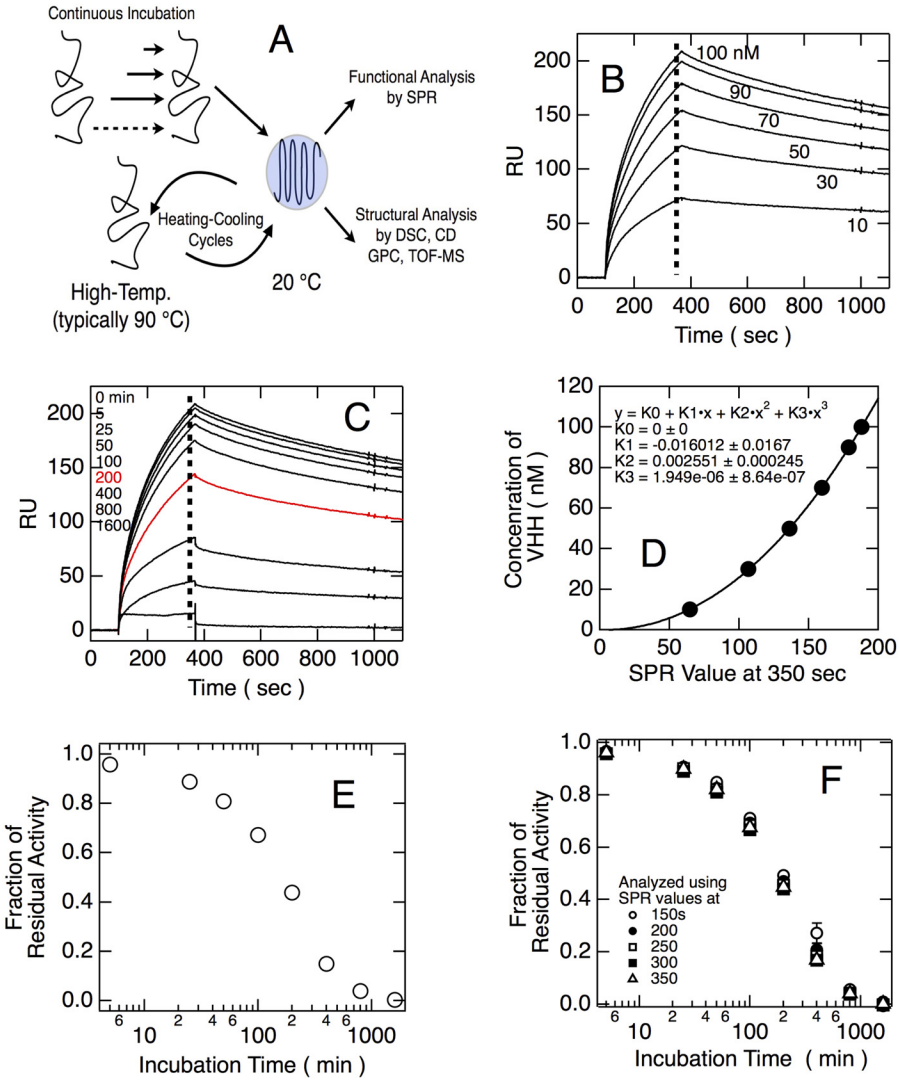

FIGURE 1. **Experimental design and determination of residual antigen binding activity.** *A*, the samples were subjected to heating-cooling cycles or continuous incubation as heat treatment. The high temperature (*High-Temp*) condition was typically 90 °C. All samples were allowed to cool to 20 °C, and their functional and structural properties were examined. *B*, typical SPR measurements obtained for standard curves. The *broken line* indicates the point at 350 s. *C*, SPR measurements of samples (1.3 μg/ml; 100 nM) treated with a continuous incubation at 90 °C for a given time. The *broken line* indicates the point at 350 s. *D*, standard curve constructed by plotting protein concentrations against SPR values at 350 s obtained in *B*. The fourth dimension polynomial fitting parameters were calculated and are indicated at the *top left* of the panel. *E*, fractions of residual activity at each time point were estimated from the SPR value at 350 s in *C* and the parameters obtained in *D*. *F*, to validate the analysis method for evaluation of the heat-induced inactivation of antibody using SPR spectra, the fractions of residual activities were estimated by using the SPR values at 150, 200, 250, 300, and 350 s. *Error bars* represent S.D. In *B*, *C*, *D*, *E*, and *F*, results of the histidine-tagged wild-type anti-hCG VHH purified from inclusion bodies are presented as a representative example. *GPC*, gel permeation chromatography; *RU*, resonance units.

A Unimolecular Reaction Was Responsible for the Irreversible Denaturation of VHH—The elimination of active VHH by heat treatment can be simulated by a single exponential equation: Fraction of residual activity = $\exp(-k_{den} \times$ Time or Cycles) where k_{den} is the first-order kinetic constant of denaturation (Fig. 2*A*). The agreement between empirical data and the first-order kinetic curve suggested that heat-induced irreversible denaturation of VHH could be approximated by a first-order reaction kinetic.

VHH heat-induced irreversible denaturation was only slightly dependent on protein concentration (range tested, 0.6 μg/ml to 1.3 mg/ml) (Fig. 4*A*). The marginal effect of protein concentration indicated that heat-induced denaturation resulted mainly from a unimolecular reaction and not from aggregation of the proteins. The proteins were subjected to 40 cycles in which ~40% of the antigen binding affinity remained (Fig. 2*A*).

Even in conditions where VHH completely lost its antigen binding activity, a considerable amount of VHH monomers was observed by analytical gel permeation chromatography (Fig. 4*B*). Samples treated with 40 heating-cooling cycles exhibited mainly a monomeric single peak in gel permeation chromatography analysis, although the peak height was 60% that of untreated VHH. VHH lost most of its activity when treated for 1,600 min at 90 °C (Fig. 2*A*). Conversely, the peak corresponding to monomeric VHH was still observed, and the height of this peak was ~25% that of untreated VHH (Fig. 4*B*). SDS-PAGE of the heat-treated sample exhibited a smeared band with the same mobility of monomeric VHH; no other bands were observed on the gel (Fig. 4*C*). These results further indi-

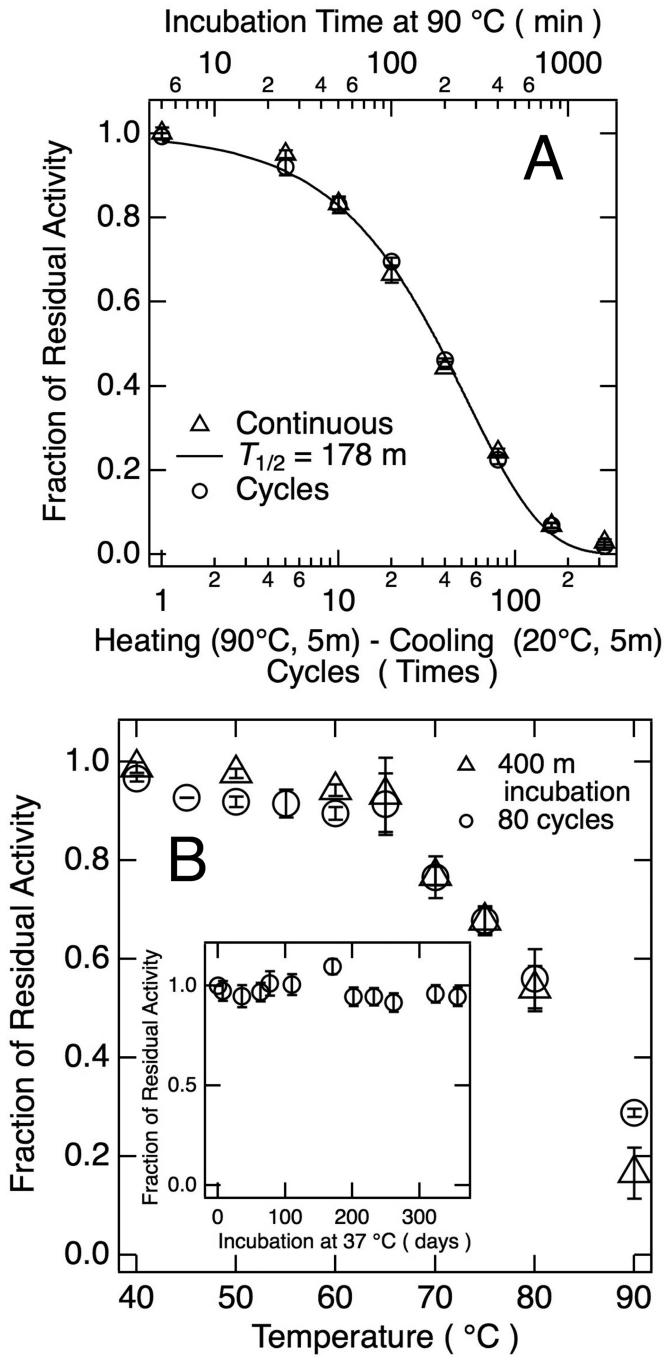

FIGURE 2. **Heat-induced irreversible denaturation of anti-hCG VHH by repetitive heating-cooling cycles or continuous incubation at a high temperature and denaturation temperature dependence.** *A*, anti-hCG VHH (1.3 μg/ml) was subjected to heating-cooling cycles (*circles*) or continuous incubation at 90 °C (*triangles*). The experiments were carried out at pH 7.4 in HBS-EP buffer. In heating-cooling cycles, a given number of reaction segments, which consisted of heating at 90 °C for 5 min and cooling at 20 °C for 5 min, were repeated. Residual activity at 20 °C was estimated using the strength of SPR signals compared with that of SPR signals from a series of diluted, untreated samples and was expressed as a fraction of the corresponding diluted, untreated sample. Because the time for unfolding was 5 min, one cycle corresponded to 5 min of incubation. The *solid line* represents a single exponential curve fitted to the VHH time-dependent denaturation where the first-order kinetic constant k_{den} was 0.0039 min^{-1} and the time to reach half of the original activity was calculated to be 178 min. *B*, VHH (1.3 μg/ml) was subjected to 80 heating-cooling cycles (*circles*) or continuous incubation (400 min (*m*); *triangles*) where the heating temperature ranged from 40 to 90 °C in HBS-EP buffer. *Inset*, VHH (1.3 μg/ml) was incubated at 37 °C for the indicated time in HBS-EP buffer. In all panels, *error bars* represent S.D.

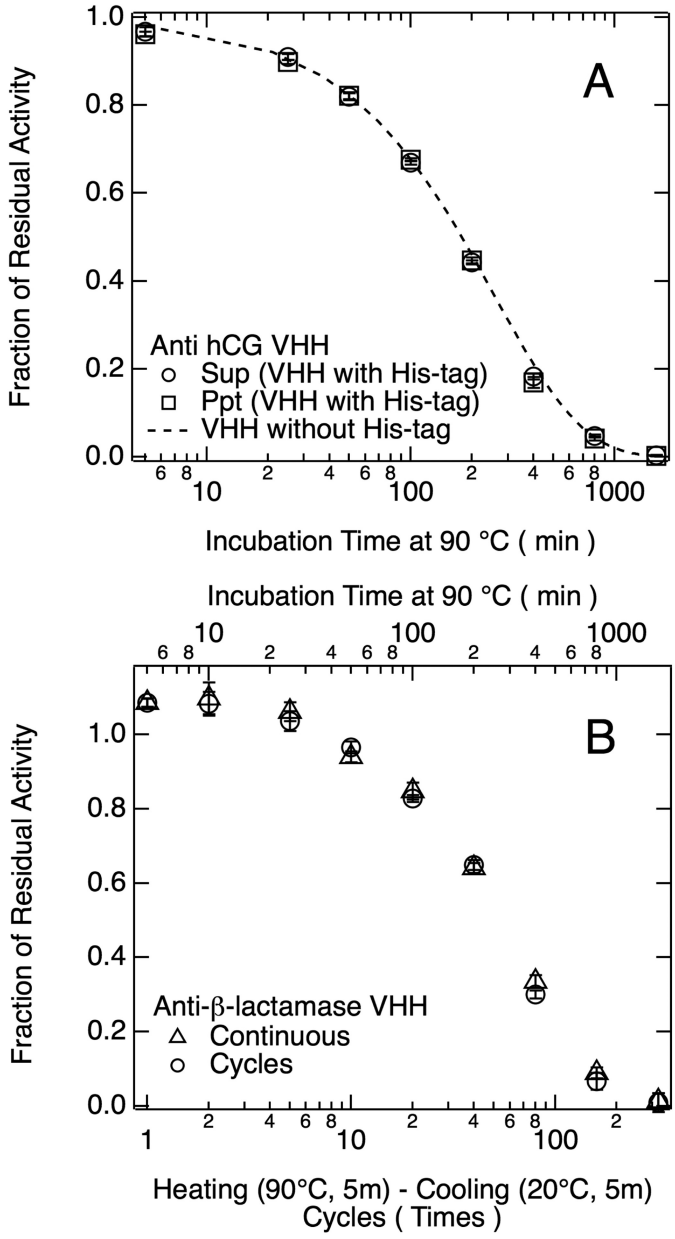

FIGURE 3. **Heat resistance of anti-hCG VHH with different preparations and anti-β-lactamase VHH.** *A*, anti-hCG VHH samples prepared from *E. coli* soluble (*circles*) and insoluble (*squares*) fractions were subjected to continuous incubation at 90 °C. Both samples were histidine-tagged at their C termini. *B*, anti-β-lactamase VHH was subjected to heating-cooling cycles (*circles*) or continuous incubation at 90 °C (*triangles*). In heating-cooling cycles, a given number of reaction segments, which consisted of heating at 90 °C for 5 min (*m*) and cooling at 20 °C for 5 min, were repeated. Both experiments were carried out at pH 7.4 in HBS-EP buffer at a protein concentration of 1.3 μg/ml. *Error bars* represent S.D. *Sup*, supernatant; *Ppt*, precipitate.

cated that irreversible denaturation of VHH occurred, at least in part, through a unimolecular reaction.

Chemical Modifications Caused the Irreversible Denaturation of VHH—Because the heat-induced irreversible denaturation of VHH involved a unimolecular process, we hypothesized that chemical modifications of amino acids and/or monomeric misfolded structures with noncovalent interactions may be related. The latter was excluded by treatment of the inactivated proteins with a high concentration of denaturant, which is thought to destroy aberrant interactions in mono-

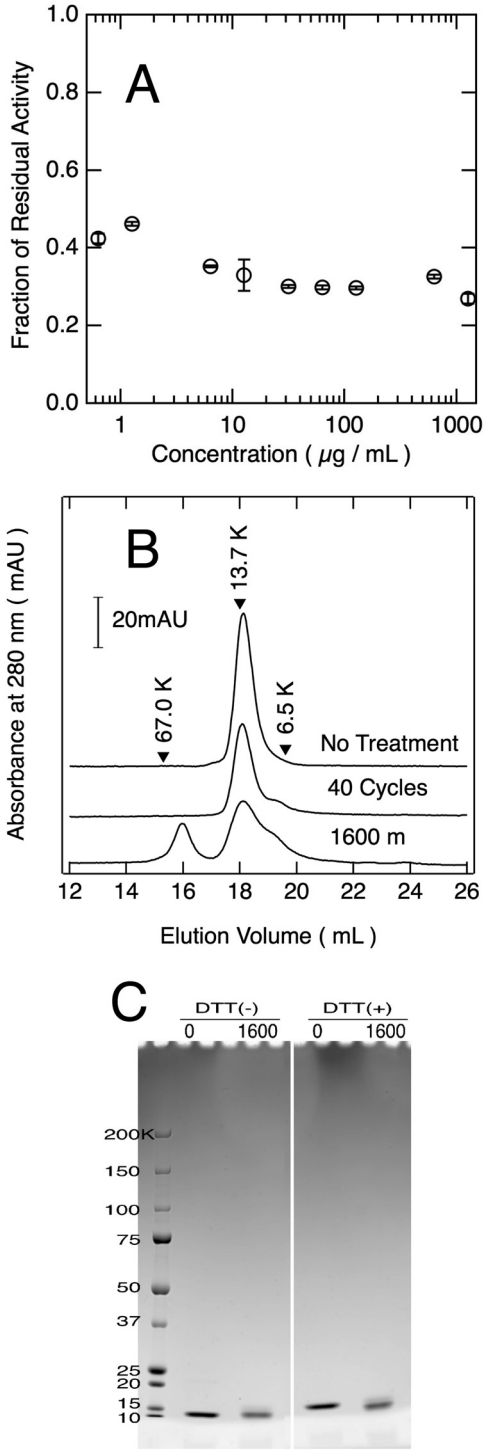

FIGURE 4. **Effects of protein concentration on VHH denaturation and analysis of the molecular weight of heat-inactivated anti-hCG VHH by gel permeation chromatography and SDS-PAGE.** *A*, VHH with different concentrations in HBS-EP buffer were subjected to 40 cycles of heating-cooling cycles (unfolding at 90 °C for 5 min and refolding at 20 °C for 5 min). *Error bars* represent S.D. *B*, room temperature gel permeation chromatography profiles of VHH without heat treatment, with 40 cycles of heating-cooling cycles, and with continuous incubation at 90 °C for 1,600 min (*m*) at a protein concentration of 10 μM. *Arrowheads* indicate the elution volumes of serum albumin (67 kDa), ribonuclease A (13.7 kDa), and trypsin inhibitor (6.5 kDa). *C*, VHH (10 μM) was treated with continuous incubation at 90 °C for 1,600 min and analyzed using a polyacrylamide gradient gel (5–20%) with or without reduction with 10 mM dithiothreitol. The *numbers* on the *left* of the panel indicate the molecular weights of marker proteins. *mAU*, milliabsorbance units.

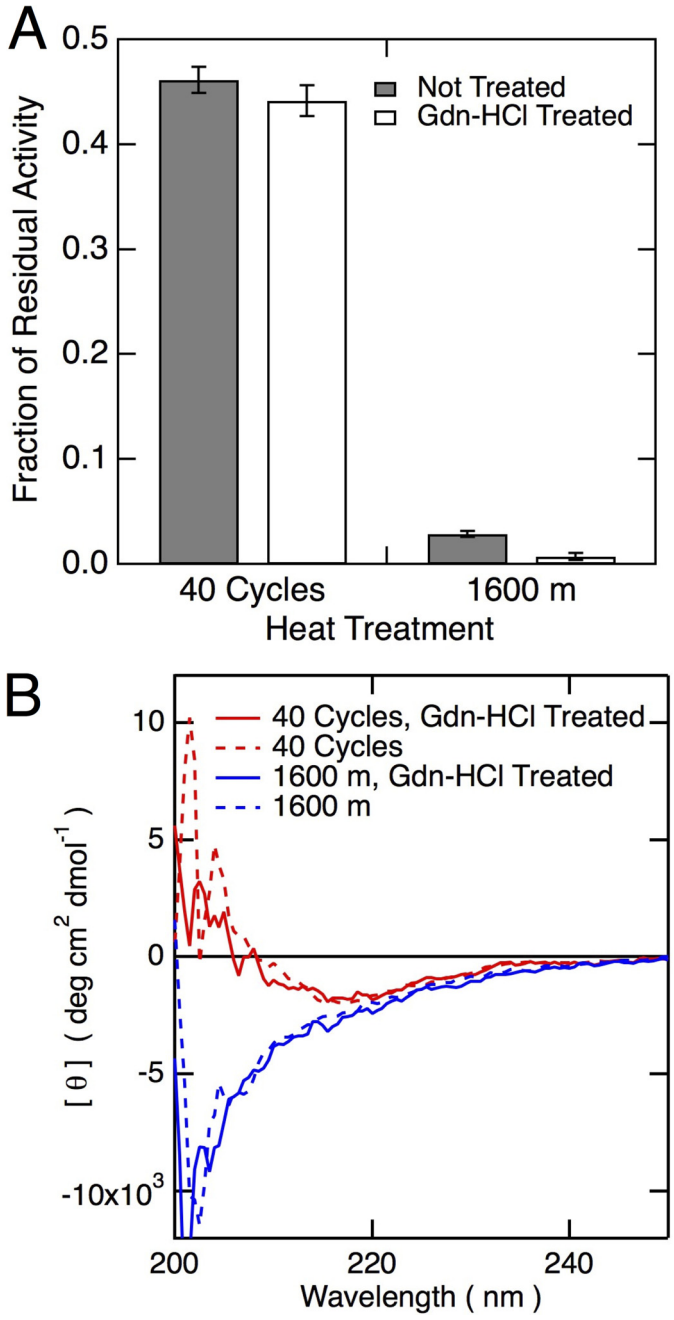

FIGURE 5. **Effects of a denaturant on heat-inactivated anti-hCG VHH.** *A*, the amount of residual activity after Gdn-HCl treatment was estimated and compared with that of VHH without Gdn-HCl treatment. Samples (40 μM) were unfolded using a final concentration of ~6 M Gdn-HCl and then dialyzed against HBS-EP buffer without EDTA to remove the denaturant. *Error bars* represent S.D. *B*, comparison of CD spectra of heat-inactivated samples at 37 °C with or without ~6 M Gdn-HCl treatment followed by refolding. *m*, minutes; *deg*, degrees.

meric misfolded structures. Samples were unfolded with ~6 M Gdn-HCl and then refolded by extensive dialysis. Gdn-HCl treatment did not result in the recovery of VHH antigen binding activity after 40 heating-cooling cycles or 1,600-min heat treatment (Fig. 5*A*). In addition, CD spectra of these samples were unchanged by Gdn-HCl treatment (Fig. 5*B*).

The mass spectra of the samples subjected to 40 cycles of heating-cooling or continuous incubation for 1,600 min exhibited a peak at a position similar to the molecular weight of

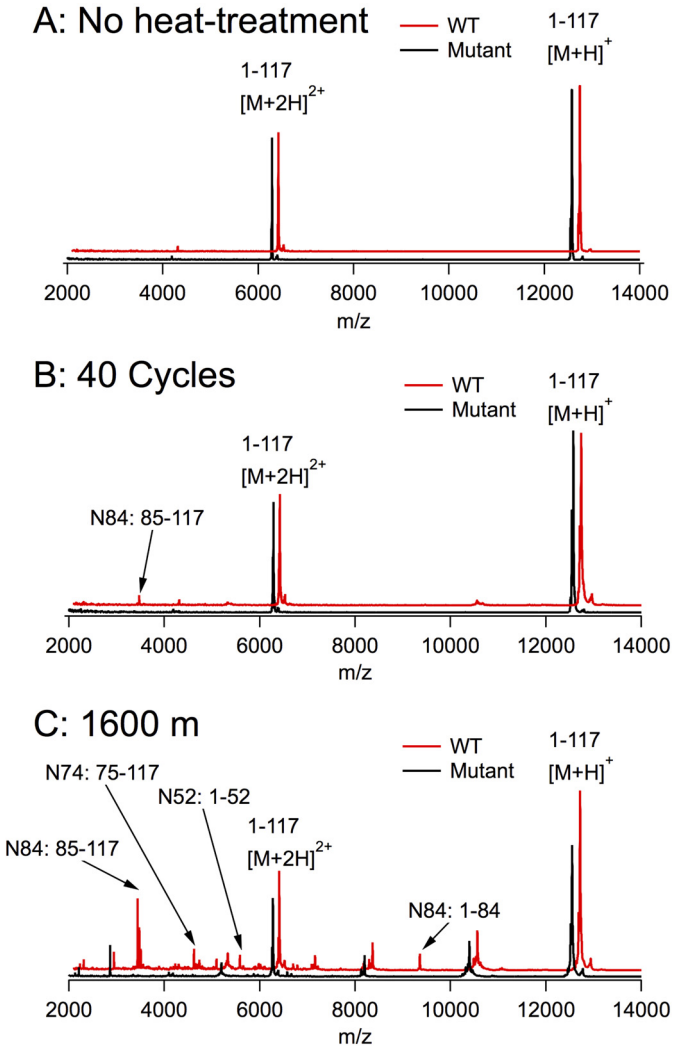

FIGURE 6. **MALDI-TOF mass spectra of wild-type and N52S/N74S/N84T mutant anti-hCG VHH with and without heat treatment.** *A*, MALDI-TOF mass spectra of wild-type (*red*) and N52S/N74S/N84T mutant (*black*) VHH (5 μM). *B* and *C*, samples were subjected to 40 heating-cooling cycles (*B*) or continuous 1,600-min (*m*) incubation (*C*) in HBS-EP buffer. The heating temperature was 90 °C. The spectra of wild-type VHH are presented with an offset of 200 *m/z* for clarity. The *arrows* indicate hypothetical fragments resulting from digestion occurring at the C terminus of Asn residues. In all panels, wild-type and N52S/N74S/N84T mutant VHH are abbreviated as *WT* and *Mutant*, respectively.

untreated VHH (12, 641) (Fig. 6). Thus, chemical modifications such as deamidation, racemization, and/or isomerization of amino acid residues were considered as potential mechanisms of denaturation because they induce only minor changes in molecular weight. These chemical reactions are often observed on Asn (1, 41–45); therefore, a VHH mutant with all Asn residues substituted by other amino acids (N52S/N74S/N84T) was prepared to evaluate the effects of chemical modifications on heat-induced denaturation (Fig. 7*A*). The VHH positions 52, 74, and 84 used here correspond to positions 52, 73, and 82a in the Kabat numbering scheme (46) and positions 57, 82, and 92 in the IMGT numbering scheme (47), respectively. After heat treatment, several extra peaks with low molecular weights were observed. Some of these extra peaks were eliminated by the replacement of Asn residues (Fig. 6, *B* and *C*). Asn residues are known as hot spots for nonenzymatic peptide bond cleavage at neutral to alkaline pH (43, 45). These peaks may represent fragments generated by cleavage at the C terminus of Asn residues, although *m/z* values were smaller by ~30–60 than the calculated molecular weight.

The N52S/N74S/N84T mutant exhibited ~50% increased half-life (274 min) against heat treatment compared with wild-type VHH (178 min) (Fig. 7*B*). Although position Asn-52 belongs to the complementarity determining region 2, the N52S/N74S/N84T mutant had an antigen binding affinity comparable with that of wild-type VHH (Fig. 7*B*, *inset*). Similar to wild-type VHH, heating-cooling cycles and continuous incubation denaturation curves were identical for the mutant as well. Thus, the incubation time at 90 °C was a critical factor determining the irreversible denaturation of the mutant.

Secondary structures of wild-type VHH and N52S/N74S/N84T were almost identical at 37 °C (Fig. 8*A*). However, the thermodynamic stability of N52S/N74S/N84T was slightly higher than that of wild-type VHH (Fig. 8*B*). The difference in T_m between these two proteins was estimated to be 3 °C. Although the T_m of a previously described mutant, C22W/A49C/I70C/C96A, was ~8 °C lower than that of wild-type VHH (33), its residual activity after 40 cycles of heat treatment was comparable with that of wild-type VHH (Fig. 8*C*). To our surprise, a highly stable mutant with an additional disulfide bond, A49C/I70C (31, 33), had markedly lower heat tolerance than wild-type VHH. These results suggested that the effects of equilibrium thermodynamic stability against heat-induced irreversible denaturation were not significant in our experimental conditions. Thus, the increase in tolerance against heat-induced irreversible denaturation of the N52S/N74S/N84T mutant occurred as a result of reduced chemical modifications.

Structural Analysis of the Heat-induced Irreversible Denaturation of VHH—Iterative DSC experiments on samples with and without heat treatment revealed a gradual decrease in the main heat absorption peak with an increase of the number of heating cycles (Fig. 9*A*). This DSC experiment was carried out without replacing the sample solution from the sample cell to avoid perturbation of the baseline; therefore, we could compare the effects of repetitive heating on C_p values. At a high temperature (85 °C), the C_p values slightly decreased with the increase in the number of heating cycles (Fig. 9*B*), indicating that heat treatment barely altered the thermodynamic characteristics of the unfolded structure. Conversely, at 35 °C, C_p values gradually increased and reached a C_p similar to that of high temperatures. This could be explained by the accumulation of unfolded structures at low temperatures because of the heat treatment. Broad but distinct heat absorption spectra were observed at ~50 °C in samples that were subjected to 20 and 30 unfolding and refolding cycles. These results indicated that heat treatment reduced the amount of proteins with intact native structures and affected the thermodynamic stability represented by the T_m in addition to affecting the folding ability. A single exponential equation fitted the change of C_p values at 63 °C against the number of measurements, suggesting that the decrease of proteins in the native state was a unimolecular reaction.

The reduction in the amount of the native state did not correlate with the residual antigen binding activity (Fig. 10, *A* and *B*). To directly compare the amount of protein in the native

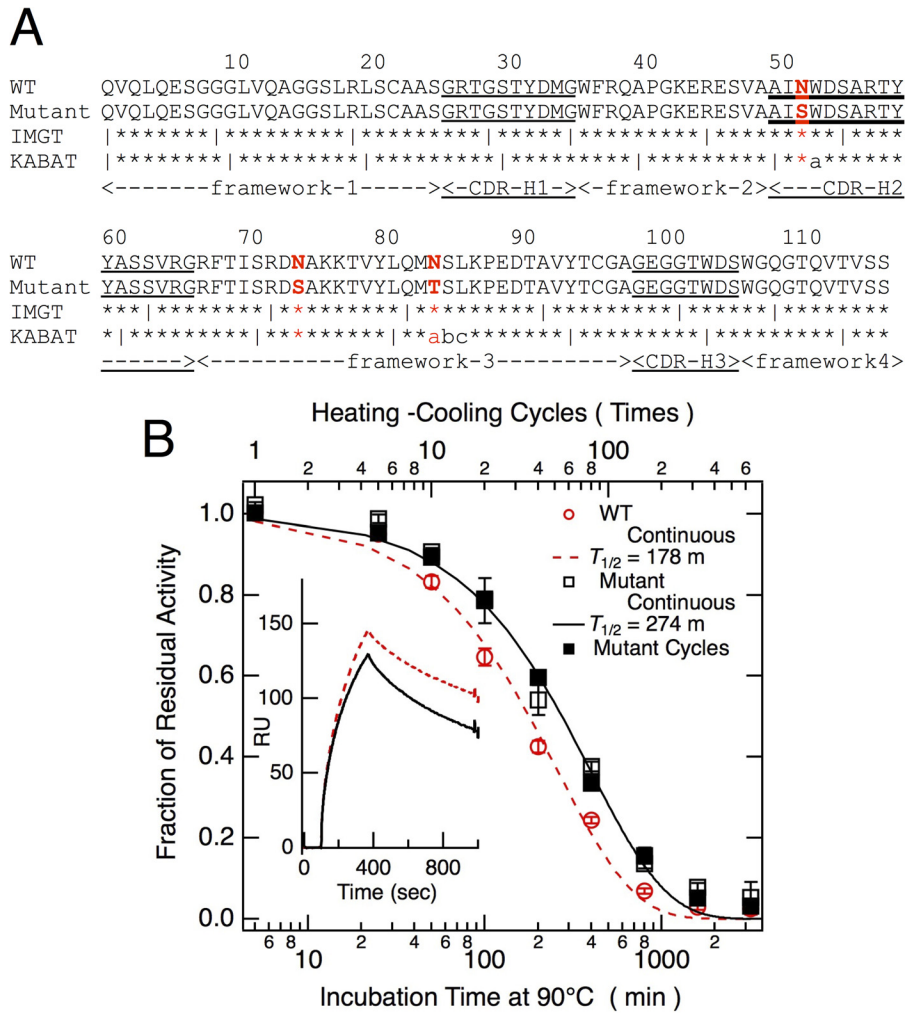

FIGURE 7. **Effects of replacement of Asn residues in anti-hCG VHH.** *A*, Asn residues 52, 74, and 84 in anti-hCG VHH-H14 were substituted by Ser, Ser, and Thr, respectively, resulting in the N52S/N74S/N84T mutant. *B*, N52S/N74S/N84T mutant (100 nM) was treated with heating (90 °C for 5 min)-cooling (20 °C for 5 min) cycles (*black closed box*) or continuous incubation at 90 °C followed by refolding at 20 °C for 5 min (*black open box*). The theoretical curve for N52S/N74S/N84T (*solid line*) was fitted using 0.0025 min^{-1} as a first-order kinetic constant k_{den}. From this k_{den}, the half-life of the N52S/N74S/N84T mutant was calculated to be 274 min (*m*). Data for wild-type VHH treated with continuous incubation and its theoretical curve are presented as *red circles* and *broken line*, respectively. The SPR signals for untreated wild-type (*red broken line*) and N52S/N74S/N84T (*black solid line*) VHHs (100 nM) are presented in the *inset*. In all panels, wild-type and N52S/N74S/N84T mutant VHHs are abbreviated as *WT* and *Mutant*, respectively. *Error bars* represent S.D. *CDR*, complementarity determining region.

state and the residual activity, samples were processed using the same methods as described above to measure their activity. Heating-cooling cycles were conducted outside of the DSC cell using a thermal cycler, and a single run of thermal unfolding for each heat-treated sample was measured using DSC (Fig. 10*A*). The heights of the main peaks in the DSC curves, which corresponded to the amount of the VHH with an intact native structure, were compared with the residual activity estimated by SPR analysis (Fig. 10*B*).

The effects of heat treatment on VHH secondary structure were investigated using CD. The sample preparation for CD experiments was identical to the sample preparation for residual activity measurements where the samples were subjected to heating (90 °C for 5 min)-cooling (20 °C for 5 min) cycles. At 37 °C, VHH secondary structure was reduced as the number of heating-cooling cycles increased using the thermal cycler (Fig. 10*C*). CD spectra from samples treated for less than 10 cycles were similar to each other. As the number of cycles increased, the CD spectra gradually changed. Although a quantitative estimation of the amount of secondary structures was difficult, more than half of the secondary structures seemed to remain after 40 cycles in contrast to the native state fraction, which was 20% when treated in the same conditions as shown for DSC (Fig. 10*B*). After 160 and 320 cycles, spectra similar to that of the thermally unfolded state at 90 °C were observed, suggesting that repetitive heating-cooling cycles resulted in the inability of VHH to refold at physiological temperature. VHH thermal unfolding curves with and without heat treatment followed by ellipticity at 235 nm indicated that the cooperativity of unfolding curves decreased with the increase in the number of heating-cooling cycles (Fig. 10*D*). This change in cooperativity was consistent with the result obtained by DSC, indicating that heat treatment decreased thermodynamic equilibrium stability and generated heterogeneous VHH molecules with various thermodynamic equilibrium stabilities.

Denaturation of Other Antibody Fragments—To examine whether the denaturation of other antibody fragments occurred via a unimolecular reaction similar to VHH, we investi-

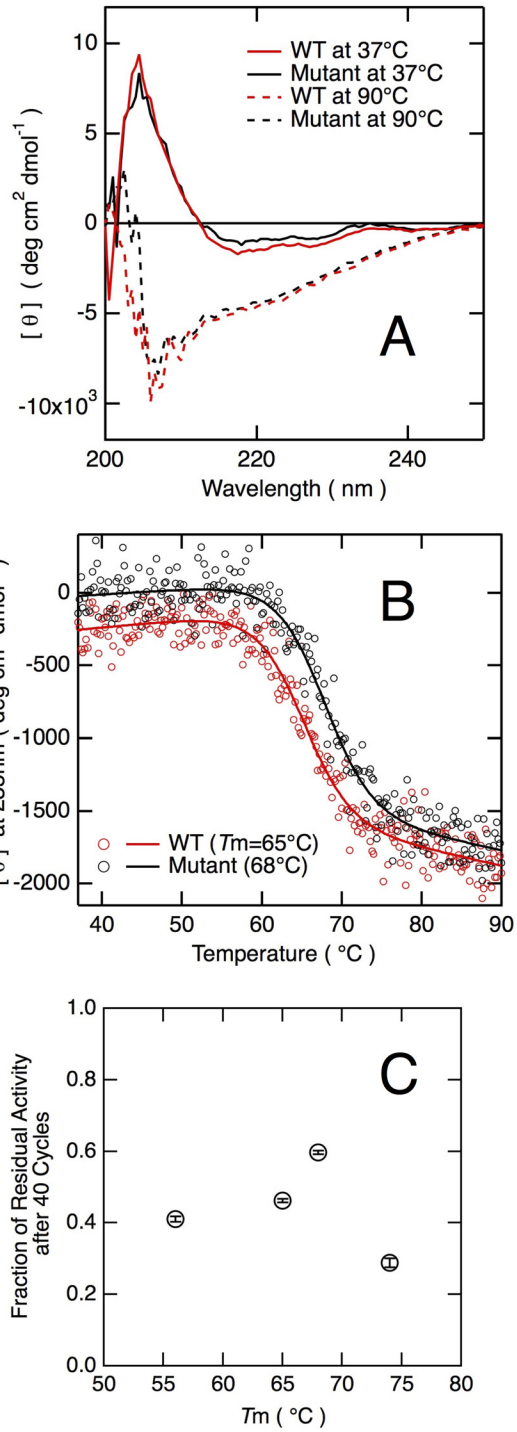

FIGURE 8. **Effects of mutations of anti-hCG VHH on its biophysical characteristics.** *A*, CD spectra of wild-type and N52S/N74S/N84T VHH (25 μM) at 37 and 90 °C in HBS-EP buffer without EDTA. *B*, equilibrium thermal unfolding curves of wild-type and N52S/N74S/N84T VHH were measured by changes in ellipticity at 235 nm at a protein concentration of 25 μM. Curves fitted by standard thermodynamic equations (63) are presented as *solid lines*, and T_m values of wild-type VHH and N52S/N74S/N84T mutant VHH were estimated to be 65 and 68 °C, respectively. *C*, T_m values and residual activities of wild-type VHH and VHH mutants (100 nM) after 40 heating-cooling cycles. The T_m values of disulfide mutants C22W/A49C/I70C/C96A (56 °C) and A49C/I70C (74 °C) are from Hagihara *et al.* (33). Wild-type and N52S/N74S/N84T mutant anti-hCG VHH are abbreviated as *WT* and *Mutant*, respectively. *Error bars* represent S.D. *deg*, degrees.

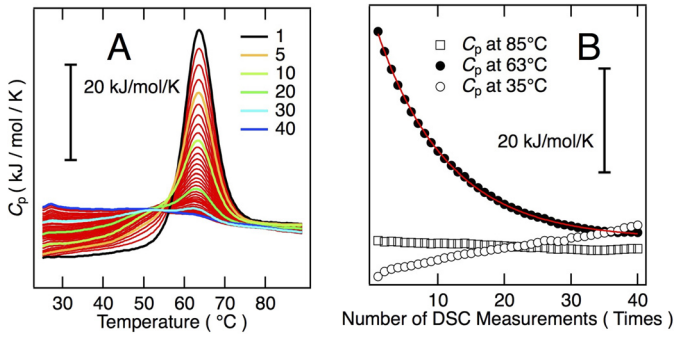

FIGURE 9. **Structural changes in anti-hCG VHH induced by iterative DSC measurements.** *A*, repetitive thermal unfolding and refolding in HBS-EP buffer induced changes in the heat absorption profiles of VHH at 54 μM. This experiment was carried out in a fixed cell without removing the samples from the DSC equipment. Heat absorption curves were measured while increasing the temperature at a rate of 1 °C/min. *B*, changes in C_p at 35 (*open circles*), 63 (*closed triangles*), and 85 °C (*open squares*) induced by repetitive DSC measurements.

gated the heat-induced denaturation of one scFv, three Fabs (Fig. 11, *A* and *B*), and their parental IgGs as controls (Fig. 11*C*). All of these antibody fragments and IgGs bound to hCG. First, the effects of heating-cooling cycles were assessed. The antigen binding activity of scFv was ~50% that of untreated scFv after the first heating-cooling cycle and gradually decreased as the heating-cooling cycle number increased (Fig. 11*A*). The Fabs showed a slightly stronger tolerance against denaturation by heating-cooling cycles than parental IgGs (Fig. 11*B*). Even after the first heating-cooling cycle, only a trace level of active antibody remained in the cases of IgG clone 28A4 and IgG clone 77F12 (Fig. 11*C*). In contrast, IgG clone 207 was more resistant to denaturation by heat treatment.

Because the residual activity after the first cycle was too low for Fabs, only scFv was used for further analysis. Consistent with the results observed for VHH, the incubation time at 90 °C, but not the number of cycles, had a dominant effect on the denaturation of scFv. However, the heat-induced irreversible denaturation of scFv depended on the protein concentration (Fig. 11*D*). Our results indicated that scFv denaturation was mainly caused by aggregation at high temperatures. In addition, the denaturation curves suggested that scFv denaturation did not proceed through a unimolecular reaction. If the denaturation is a unimolecular reaction and 50% of activity is lost in each cycle or every 5 min, then less than 5% of scFv activity would remain after five cycles or 25 min of treatment; this value was estimated by the fifth power of 0.5. However, our experiment showed that 30% of the initial activity of scFv was present after five cycles or 25 min. The dependence of scFv denaturation on heating temperature was different from that of VHH (Fig. 11*D*, *inset*). In contrast to the monophasic dependence of VHH, the residual activity of scFv after seven cycles of heat treatment was lowest at 80 °C and slightly increased with the increase in heating temperature. Denaturation of both VHH and scFv started between 65 and 70 °C.

DISCUSSION

VHH folding/unfolding intermediates were not dominant factors for heat-induced irreversible denaturation. Our experimental results suggested that VHH denaturation was mainly

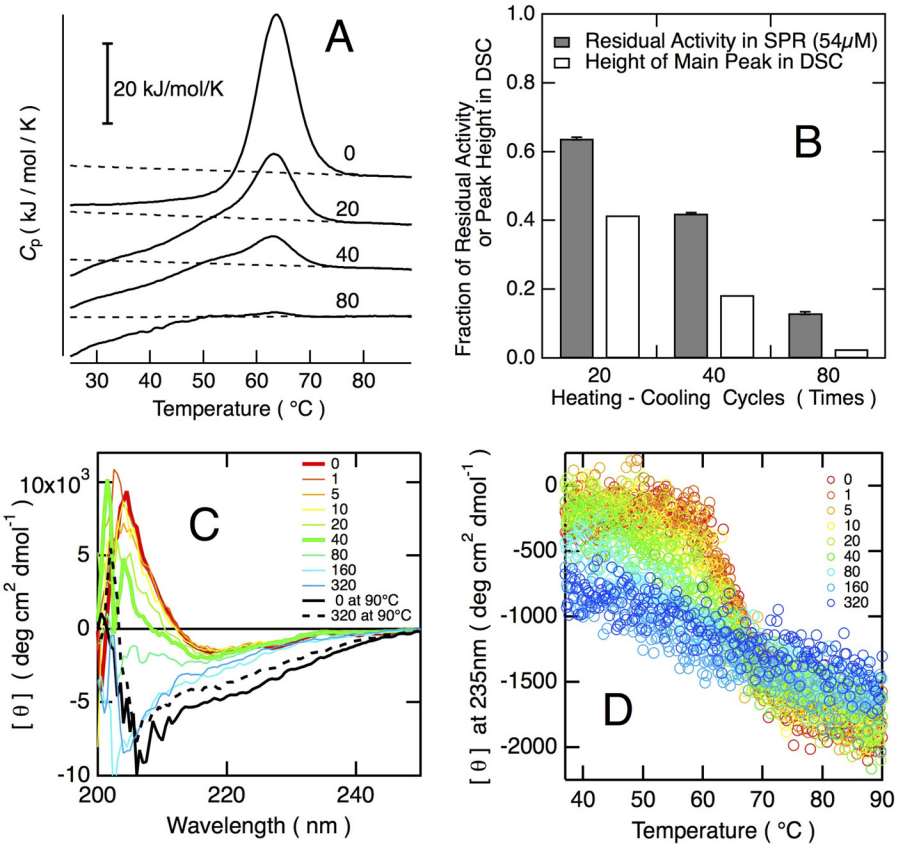

FIGURE 10. **Comparison of heat-induced structural changes and denaturation of anti-hCG VHH.** *A*, VHH heat absorption curves. VHH samples (54 μM in HBS-EP buffer) were subjected to cycles of unfolding at 90 °C for 5 min and refolding at 20 °C for 5 min in a thermal cycler. The *broken lines* represent the extrapolated linear baseline of the unfolded state. The number of cycles is indicated on each curve. *B*, comparison between residual activities measured by SPR and the main peak of heat absorption curves corresponding to intact VHH after heat treatment. The main peaks were estimated by subtracting the baseline (unfolded state) from the peak heights for all samples, and the resulting heat-treated peak was then divided by the untreated sample peak. *Error bars* represent S.D. *C*, CD spectra of heat-treated VHH at 37 °C in HBS-EP buffer without EDTA. Samples at a protein concentration of 25 μM were subjected to cycles of unfolding at 90 °C for 5 min and refolding at 20 °C for 5 min. For comparison, CD spectra of thermally unfolded intact and heat-denatured VHH at 90 °C are also shown. *D*, equilibrium thermal unfolding curves of heat-treated VHH measured by changes in ellipticity at 235 nm. Samples were the same as in *C*. *deg*, degrees.

due to chemical modifications of amino acids because denaturation occurred as a unimolecular reaction irrelevant of the presence of misfolded monomers and because Asn replacement increased VHH heat resistance. Various chemical modifications are often induced by heat in many proteins, and these modifications are supposed to be an important factor for protein denaturation. However, chemical modifications are rarely found to be a major driving force of heat-induced irreversible denaturation mainly because a number of proteins are inactivated by mixed effects of chemical modifications and aggregation, which are difficult to discriminate. Although lysozyme (19, 21) and ribonuclease A (24, 48) are denatured by chemical modifications at high temperatures, the importance of their folding/unfolding intermediates on the entire process of denaturation remains to be elucidated. Precise discrimination between the effects of folding/unfolding intermediates and other factors was achieved in this work by comparing the impacts of heating-cooling cycles and continuous incubation at high temperature.

VHH heat-induced irreversible denaturation followed first-order kinetics, and the concentration of VHH did not significantly alter the residual activity of VHH after heat treatment. Even after the antigen binding ability of VHH was almost completely lost, considerable amounts of monomeric VHH still remained. In addition, repetitive unfolding experiments by DSC revealed that a fraction of intact natively structured molecules decreased according to first-order kinetics. These data indicated that the unimolecular reaction caused by heat treatment dominantly affected VHH physical properties. Similar to VHH, heat-induced irreversible denaturation of lysozyme (21), ribonuclease A (48), and ovalbumin (49) was reported to be independent of protein concentration. The unimolecular reaction inducing the irreversible denaturation can be caused by chemical modifications and/or the generation of misfolded monomers (11). In the case of VHH, the presence of monomeric misfolded molecules was unlikely because the treatment of inactivated VHH with a denaturant that loosens misfolded structures did not allow recovery of the antigen binding activity and its secondary structure.

Asn residues are susceptible to various chemical modifications (1, 41–45). We found that the N52S/N74S/N84T mutant was more resistant to heat-induced irreversible denaturation than the wild-type VHH protein, suggesting the importance of chemical modifications for VHH heat resistance. Ahern *et al.* (25) also reported that replacement of Asn residues increased the tolerance of triose-phosphate isomerase to heat. The Asn mutations reduced protein fragmentation, indicating that these residues were indeed chemically modified in our experimental

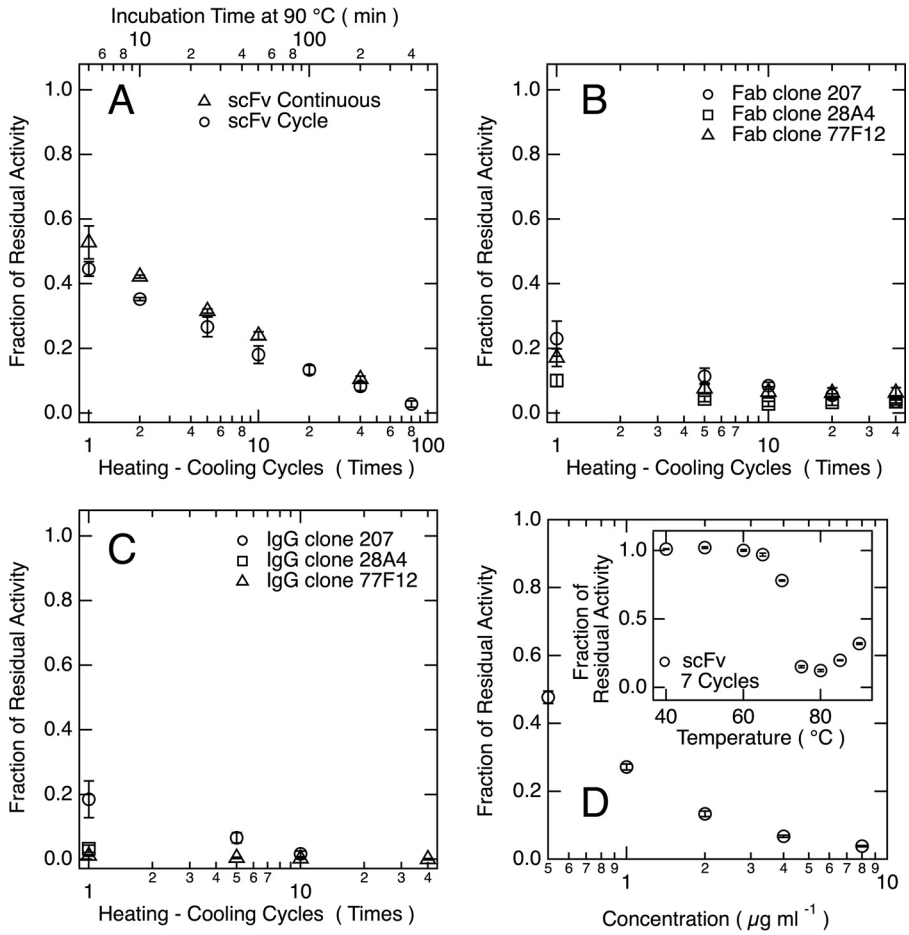

FIGURE 11. **Heat-induced irreversible denaturation of anti-hCG antibody fragments.** *A–C*, scFv (*A*), Fab (*B*), and IgG (*C*) samples (1 μg/ml) were subjected to heating (90 °C for 5 min)-cooling (20 °C for 5 min) cycles at pH 7.4. In addition, dependence of scFv denaturation on incubation time at 90 °C is also shown (*A*). Residual activity at 20 °C was estimated using the strength of the SPR signal compared with that of SPR signals from a series of diluted untreated samples and is presented as the fraction of the corresponding untreated diluted sample. *D*, concentration-dependent denaturation of scFv was examined. ScFv samples with the given concentrations were subjected to five cycles of unfolding at 90 °C for 5 min and refolding at 20 °C for 5 min. *Inset*, scFv (1 μg/ml) was subjected to seven heating-cooling cycles where the heating temperatures ranged from 40 to 90 °C in HBS-EP buffer. *Error bars* represent S.D. in all panels.

conditions. Both deamidation and peptide bond cleavage cause succinimide formation, and the former is followed by spontaneous isomerization and racemization (43, 45). Using the hexapeptide VYPNLA, Geiger and Clarke (43) demonstrated that heat treatment at 100 °C and pH 7.4 resulted in 64% isopeptides, 22% normal peptides in which Asn was modified to Asp, and 14% tetrapeptide cleavage products. Fragmentation indicates the occurrence of deamidation-related modifications, which are approximately 7 times more frequent than fragmentation itself.

Heat treatment decreased the stability and folding ability of VHH as revealed by CD and DSC. The first-order kinetic model fitted the decrease of the native state by iterative DSC measurements, and treatment with the denaturant did not allow recovery of secondary structures of denatured VHH. Therefore, these changes in physical properties were thought to originate from chemical modifications. Interestingly, the residual fraction of intact native VHH was smaller than the residual fraction of antigen binding activity. This result indicated that both native VHH and some of the VHH molecules deteriorated by heat treatment could maintain their antigen binding ability. The presence of folded and functional molecules with reduced thermodynamic stability was supported by our CD experiments where the amount of secondary structure may be less sensitive than the amount of protein in the intact native structure. Two pathways can explain VHH denaturation by chemical modifications. In the first pathway, accumulation of chemical modifications may induce gradual loss of stability and folding ability, which in turn lead to denaturation. The second pathway may involve modifications of a smaller number of specific amino acids that are critical for antigen binding activity, such as amino acids located in the *complementarity determining* region.

From CD and DSC experiments, the chemical modifications are suggested to affect the native structure of VHH; *i.e.* the chemically modified amino acids alter atomic interactions found in the native structure. Side chains of Asn residues were largely exposed to the solvent in the crystal structure (Protein Data Bank code 1HCV) (39), and the modification in the side chain may be the cause of minor effects on the structure. However, main chains were partially buried (Fig. 12, *A* and *B*). Chemical modifications, such as deamidation of Asn, also affect main chains, and thus Asn chemical modification changes the van der Waals interaction with main chain atoms and atoms of other surrounding amino acids. In addition, amides of Asn res-

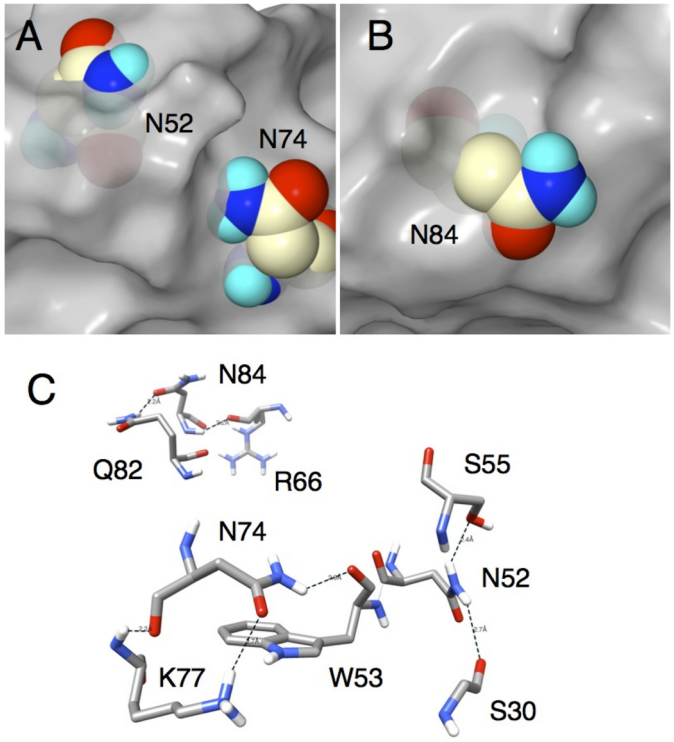

FIGURE 12. **Atomic interaction of Asn residues in the crystal structure of anti-hCG VHH.** *A* and *B*, solvent-excluded surface (*gray*) of anti-hCG VHH molecule around Asn residues, which are indicated by Corey-Pauling-Koltun model. Surface was generated by CueMol2 using Protein Data Bank code 1HCV data (39) with the probe radius of 4 Å. *C*, hydrogen bond network related to the Asn residues. Both the side chain and main chain atoms of Asn residues form hydrogen bonds with proximal atoms of other amino acid residues (*dashed line*). Hydrogen bonds were detected, and the graphic was drawn by using UCSF Chimera (64).

idues form hydrogen bonds with proximal residues (Fig. 12*C*). The chemical modifications of Asn residues alter the van der Waals interactions and hydrogen bonds of the native structure, resulting in a change in the stability and function of VHH.

Our results indicated that the mechanisms of heat-induced irreversible denaturation of scFv and VHH were different. Denaturation of scFv was affected by protein concentration and thus controlled by aggregation at high temperatures, whereas VHH denaturation depended on chemical modifications. In addition, the temperature dependence of scFv denaturation was biphasic, therefore making it different from that of VHH, which was monophasic. Both domains of scFv were thought to be unfolded at 90 °C, but it is highly possible that at least one domain is folded or partially folded at temperatures close to 75 °C (50–53). Demarest and Glaser (54) proposed that aggregation can be caused by interactions of single domains, interactions between variable heavy and variable light fragments of different molecules, and/or intermolecular tail to tail interactions of exposed base regions of domains. Although our experimental results could not discriminate among the above three factors, heterologous interactions of heavy and light chain variable domains may explain the significant differences in heat tolerance between scFv and VHH. Omidfar *et al.* (9) reported that whole camelid heavy chain antibody, which has only homogeneous interactions between heavy chains, was more stable than conventional IgG and slightly weaker than VHH, supporting our hypothesis.

Chemical modification of Asn can occur in every protein and possibly causes adverse effects. It is known that senile cataract is induced by insoluble eye lens crystallin, and Asn deamidation was found to be one of the major *in vivo* modifications of insoluble crystallin (55, 56). Formation of amyloid fibril was enhanced by deamidation of a model peptide of amylin (the human islet amyloid polypeptide) that forms amyloid deposits in type 2 diabetes mellitus (57, 58), although it is arguable whether the chemical modification generally causes amyloid diseases. In an anthrax vaccine, a spontaneous Asn deamidation of the antigen occurred during storage. It was suggested that deamidation was the cause of its reduction in effectiveness of immunogenicity (59). In addition, deamidation is responsible for much of the heterogeneity of pharmaceutically important proteins such as antibodies (1). Conversely, deamidation of food proteins, such as in whey and wheat, improves their functional properties and makes them more useful for the industry (60). Deamidation of Asn changes the net charge of food proteins and thus gives a preferable effect on the solubility at neutral pH. As well as the examples above, Asn modifications have been observed in numerous proteins (61). Quantitative evaluation of the effects of chemical modifications may give clues to control biological events and improve industrially important proteins.

By precisely analyzing the entire process of VHH heat-induced irreversible denaturation, we identified chemical modifications of amino acids as a dominant mechanism governing VHH heat resistance. Chemical modifications are easily controlled compared with aggregation, which depends on the structure of the folding intermediates and/or the unfolded state. Indeed, replacement of fragile amino acids simply increased heat tolerance as shown by the use of the N52S/N74S/N84T VHH mutant in this study. In addition, amino acid derivatives and polyamines are known to prevent heat-induced chemical modifications (62). Our findings enabled a focused optimization of parameters controlling heat-induced denaturation and will help to elevate VHH heat tolerance.

Acknowledgments—We thank Lilian Kaede Komaba for critical reading of the manuscript. A part of the molecular graphics and analyses was performed with the UCSF Chimera package. Chimera was developed by the Resource for Biocomputing, Visualization, and Informatics at the University of California, San Francisco (supported by National Institutes of Health Grant P41-GM103311 from the NIGMS).

REFERENCES

1. Manning, M. C., Chou, D. K., Murphy, B. M., Payne, R. W., and Katayama, D. S. (2010) Stability of protein pharmaceuticals: an update. *Pharm. Res.* **27,** 544–575
2. Saerens, D., Huang, L., Bonroy, K., and Muyldermans, S. (2008) Antibody fragments as probe in biosensor development. *Sensors* **8,** 4669–4686
3. Hamers-Casterman, C., Atarhouch, T., Muyldermans, S., Robinson, G., Hamers, C., Songa, E. B., Bendahman, N., and Hamers, R. (1993) Naturally occurring antibodies devoid of light chains. *Nature* **363,** 446–448
4. Muyldermans, S. (2013) Nanobodies: natural single-domain antibodies. *Annu. Rev. Biochem.* **82,** 775–797
5. van der Linden, R. H., Frenken, L. G., de Geus, B., Harmsen, M. M., Ruuls, R. C., Stok, W., de Ron, L., Wilson, S., Davis, P., and Verrips, C. T. (1999)

Comparison of physical chemical properties of llama VHH antibody fragments and mouse monoclonal antibodies. *Biochim. Biophys. Acta* **1431,** 37–46
6. Pérez, J. M., Renisio, J. G., Prompers, J. J., van Platerink, C. J., Cambillau, C., Darbon, H., and Frenken, L. G. (2001) Thermal unfolding of a llama antibody fragment: a two-state reversible process. *Biochemistry* **40,** 74–83
7. Dumoulin, M., Conrath, K., Van Meirhaeghe, A., Meersman, F., Heremans, K., Frenken, L. G., Muyldermans, S., Wyns, L., and Matagne, A. (2002) Single-domain antibody fragments with high conformational stability. *Protein Sci.* **11,** 500–515
8. Ladenson, R. C., Crimmins, D. L., Landt, Y., and Ladenson, J. H. (2006) Isolation and characterization of a thermally stable recombinant anti-caffeine heavy-chain antibody fragment. *Anal. Chem.* **78,** 4501–4508
9. Omidfar, K., Rasaee, M. J., Kashanian, S., Paknejad, M., and Bathaie, Z. (2007) Studies of thermostability in *Camelus bactrianus* (Bactrian camel) single-domain antibody specific for the mutant epidermal-growth-factor receptor expressed by *Pichia*. *Biotechnol. Appl. Biochem.* **46,** 41–49
10. Ewert, S., Cambillau, C., Conrath, K., and Plückthun, A. (2002) Biophysical properties of camelid V_{HH} domains compared to those of human V_H3 domains. *Biochemistry* **41,** 3628–3636
11. Klibanov, A. M. (1983) Stabilization of enzymes against thermal inactivation. *Adv. Appl. Microbiol.* **29,** 1–28
12. Fink, A. L. (1998) Protein aggregation: folding aggregates, inclusion bodies and amyloid. *Fold. Des.* **3,** R9–R23
13. Jahn, T. R., and Radford, S. E. (2008) Folding versus aggregation: polypeptide conformations on competing pathways. *Arch. Biochem. Biophys.* **469,** 100–117
14. Horowitz, P. M. (1993) Facilitation of protein folding and the reversibility of denaturation. *ACS Symp. Ser. Am. Chem. Soc.* **516,** 167–172
15. Wörn, A., and Plückthun, A. (2001) Stability engineering of antibody single-chain Fv fragments. *J. Mol. Biol.* **305,** 989–1010
16. Wang, W. (2005) Protein aggregation and its inhibition in biopharmaceutics. *Int. J. Pharm.* **289,** 1–30
17. Dong, A., Prestrelski, S. J., Allison, S. D., and Carpenter, J. F. (1995) Infrared spectroscopic studies of lyophilization-induced and temperature-induced protein aggregation. *J. Pharm. Sci.* **84,** 415–424
18. Le Bon, C., Nicolai, T., and Durand, D. (1999) Kinetics of aggregation and gelation of globular proteins after heat-induced denaturation. *Macromolecules* **32,** 6120–6127
19. Tomizawa, H., Yamada, H., and Imoto, T. (1994) The mechanism of irreversible inactivation of lysozyme at pH 4 and 100 °C. *Biochemistry* **33,** 13032–13037
20. Zheng, J. Y., and Janis, L. J. (2006) Influence of pH, buffer species, and storage temperature on physicochemical stability of a humanized monoclonal antibody LA298. *Int. J. Pharm.* **308,** 46–51
21. Ahern, T. J., and Klibanov, A. M. (1985) The mechanisms of irreversible enzyme inactivation at 100 °C. *Science* **228,** 1280–1284
22. Rombouts, I., Lagrain, B., Brunnbauer, M., Koehler, P., Brijs, K., and Delcour, J. A. (2011) Identification of isopeptide bonds in heat-treated wheat gluten peptides. *J. Agric. Food Chem.* **59,** 1236–1243
23. van Boekel, M. A. (1999) Heat-induced deamidation, dephosphorylation and breakdown of caseinate. *Int. Dairy J.* **9,** 237–241
24. Zale, S. E., and Klibanov, A. M. (1986) Why does ribonuclease irreversibly inactivate at high-temperatures? *Biochemistry* **25,** 5432–5444
25. Ahern, T. J., Casal, J. I., Petsko, G. A., and Klibanov, A. M. (1987) Control of oligomeric enzyme thermostability by protein engineering. *Proc. Natl. Acad. Sci. U.S.A.* **84,** 675–679
26. Zhou, Y., Lau, F. W., Nauli, S., Yang, D., and Bowie, J. U. (2001) Inactivation mechanism of the membrane protein diacylglycerol kinase in detergent solution. *Protein Sci.* **10,** 378–383
27. Renisio, J. G., Pérez, J., Czisch, M., Guenneugues, M., Bornet, O., Frenken, L., Cambillau, C., and Darbon, H. (2002) Solution structure and backbone dynamics of an antigen-free heavy chain variable domain (VHH) from llama. *Proteins* **47,** 546–555
28. Conrath, K. E., Lauwereys, M., Galleni, M., Matagne, A., Frère, J. M., Kinne, J., Wyns, L., and Muyldermans, S. (2001) β-Lactamase inhibitors derived from single-domain antibody fragments elicited in the Camelidae. *Antimicrob. Agents Chemother.* **45,** 2807–2812
29. Hagihara, Y., and Saerens, D. (2012) Improvement of single domain antibody stability by disulfide bond introduction. *Methods Mol. Biol.* **911,** 399–416
30. Saerens, D., Pellis, M., Loris, R., Pardon, E., Dumoulin, M., Matagne, A., Wyns, L., Muyldermans, S., and Conrath, K. (2005) Identification of a universal VHH framework to graft non-canonical antigen-binding loops of camel single-domain antibodies. *J. Mol. Biol.* **352,** 597–607
31. Saerens, D., Conrath, K., Govaert, J., and Muyldermans, S. (2008) Disulfide bond introduction for general stabilization of immunoglobulin heavy-chain variable domains. *J. Mol. Biol.* **377,** 478–488
32. Hagihara, Y., Matsuda, T., and Yumoto, N. (2005) Cellular quality control screening to identify amino acid pairs for substituting the disulfide bonds in immunoglobulin fold domains. *J. Biol. Chem.* **280,** 24752–24758
33. Hagihara, Y., Mine, S., and Uegaki, K. (2007) Stabilization of an immunoglobulin fold domain by an engineered disulfide bond at the buried hydrophobic region. *J. Biol. Chem.* **282,** 36489–36495
34. Doering, D. S., and Matsudaira, P. (1996) Cysteine scanning mutagenesis at 40 of 76 positions in villin headpiece maps the F-actin binding site and structural features of the domain. *Biochemistry* **35,** 12677–12685
35. Ellman, G. L. (1958) A colorimetric method for determining low concentrations of mercaptans. *Arch. Biochem. Biophys.* **74,** 443–450
36. Edelhoch, H. (1967) Spectroscopic determination of tryptophan and tyrosine in proteins. *Biochemistry* **6,** 1948–1954
37. Davies, R. B., and Abraham, E. P. (1974) Separation, purification and properties of β-lactamase I and β-lactamase II from *Bacillus cereus* 569/H/9. *Biochem. J.* **143,** 115–127
38. Dolk, E., van Vliet, C., Perez, J. M., Vriend, G., Darbon, H., Ferrat, G., Cambillau, C., Frenken, L. G., and Verrips, T. (2005) Induced refolding of a temperature denatured llama heavy-chain antibody fragment by its antigen. *Proteins* **59,** 555–564
39. Spinelli, S., Frenken, L., Bourgeois, D., de Ron, L., Bos, W., Verrips, T., Anguille, C., Cambillau, C., and Tegoni, M. (1996) The crystal structure of a llama heavy chain variable domain. *Nat. Struct. Biol.* **3,** 752–757
40. Frenken, L. G., van der Linden, R. H., Hermans, P. W., Bos, J. W., Ruuls, R. C., de Geus, B., and Verrips, C. T. (2000) Isolation of antigen specific llama VHH antibody fragments and their high level secretion by *Saccharomyces cerevisiae*. *J. Biotechnol.* **78,** 11–21
41. Stephenson, R. C., and Clarke, S. (1989) Succinimide formation from aspartyl and asparaginyl peptides as a model for the spontaneous degradation of proteins. *J. Biol. Chem.* **264,** 6164–6170
42. Zhao, M. X., Bada, J. L., and Ahern, T. J. (1989) Racemization rates of asparagine aspartic-acid residues in lysozyme at 100 °C as a function of pH. *Bioorg. Chem.* **17,** 36–40
43. Geiger, T., and Clarke, S. (1987) Deamidation, isomerization, and racemization at asparaginyl and aspartyl residues in peptides. Succinimide-linked reactions that contribute to protein-degradation. *J. Biol. Chem.* **262,** 785–794
44. Li, B., Borchardt, R. T., Topp, E. M., VanderVelde, D., and Schowen, R. L. (2003) Racemization of an asparagine residue during peptide deamidation. *J. Am. Chem. Soc.* **125,** 11486–11487
45. Patel, K., and Borchardt, R. T. (1990) Chemical pathways of peptide degradation. III. Effect of primary sequence on the pathways of deamidation of asparaginyl residues in hexapeptides. *Pharm. Res.* **7,** 787–793
46. Kabat, E. A., Wu, T. T., Perry, H. M., Gottsman, K. S., and Foeller, C. (1991) *Sequences of Proteins of Immunologic Interest*, 5th Ed., United States Department of Health and Human Services, Public Health Service, National Institutes of Health, Bethesda, MD
47. Lefranc, M. P., Pommié, C., Ruiz, M., Giudicelli, V., Foulquier, E., Truong, L., Thouvenin-Contet, V., and Lefranc, G. (2003) IMGT unique numbering for immunoglobulin and T cell receptor variable domains and Ig superfamily V-like domains. *Dev. Comp. Immunol.* **27,** 55–77
48. Zale, S. E., and Klibanov, A. M. (1983) On the role of reversible denaturation (unfolding) in the irreversible thermal inactivation of enzymes. *Biotechnol. Bioeng.* **25,** 2221–2230
49. Weijers, M., Barneveld, P. A., Cohen Stuart, M. A., and Visschers, R. W. (2003) Heat-induced denaturation and aggregation of ovalbumin at neutral pH described by irreversible first-order kinetics. *Protein Sci.* **12,** 2693–2703

50. Rodríguez-Rodríguez, E. R., Ledezma-Candanoza, L. M., Contreras-Ferrat, L. G., Olamendi-Portugal, T., Possani, L. D., Becerril, B., and Riaño-Umbarila, L. (2012) A single mutation in framework 2 of the heavy variable domain improves the properties of a diabody and a related single-chain antibody. *J. Mol. Biol.* **423,** 337–350
51. Miller, B. R., Demarest, S. J., Lugovskoy, A., Huang, F., Wu, X., Snyder, W. B., Croner, L. J., Wang, N., Amatucci, A., Michaelson, J. S., and Glaser, S. M. (2010) Stability engineering of scFvs for the development of bispecific and multivalent antibodies. *Protein Eng. Des. Sel.* **23,** 549–557
52. Weatherill, E. E., Cain, K. L., Heywood, S. P., Compson, J. E., Heads, J. T., Adams, R., and Humphreys, D. P. (2012) Towards a universal disulphide stabilised single chain Fv format: importance of interchain disulphide bond location and vL-vH orientation. *Protein Eng. Des. Sel.* **25,** 321–329
53. Kim, D. Y., Kandalaft, H., Ding, W., Ryan, S., van Faassen, H., Hirama, T., Foote, S. J., MacKenzie, R., and Tanha, J. (2012) Disulfide linkage engineering for improving biophysical properties of human VH domains. *Protein Eng. Des. Sel.* **25,** 581–589
54. Demarest, S. J., and Glaser, S. M. (2008) Antibody therapeutics, antibody engineering, and the merits of protein stability. *Curr. Opin. Drug Discov. Devel.* **11,** 675–687
55. Hanson, S. R., Hasan, A., Smith, D. L., and Smith, J. B. (2000) The major *in vivo* modifications of the human water-insoluble lens crystallins are disulfide bonds, deamidation, methionine oxidation and backbone cleavage. *Exp. Eye Res.* **71,** 195–207
56. Wilmarth, P. A., Tanner, S., Dasari, S., Nagalla, S. R., Riviere, M. A., Bafna, V., Pevzner, P. A., and David, L. L. (2006) Age-related changes in human crystallins determined from comparative analysis of post-translational modifications in young and aged lens: does deamidation contribute to crystallin insolubility? *J. Proteome Res.* **5,** 2554–2566
57. Nilsson, M. R., Driscoll, M., and Raleigh, D. P. (2002) Low levels of asparagine deamidation can have a dramatic effect on aggregation of amyloidogenic peptides: implications for the study of amyloid formation. *Protein Sci.* **11,** 342–349
58. Dunkelberger, E. B., Buchanan, L. E., Marek, P., Cao, P., Raleigh, D. P., and Zanni, M. T. (2012) Deamidation accelerates amyloid formation and alters amylin fiber structure. *J. Am. Chem. Soc.* **134,** 12658–12667
59. Verma, A., McNichol, B., Domínguez-Castillo, R. I., Amador-Molina, J. C., Arciniega, J. L., Reiter, K., Meade, B. D., Ngundi, M. M., Stibitz, S., and Burns, D. L. (2013) Use of site-directed mutagenesis to model the effects of spontaneous deamidation on the immunogenicity of *Bacillus anthracis* protective antigen. *Infect. Immun.* **81,** 278–284
60. Riha, W. E., 3rd, Izzo, H. V., Zhang, J., and Ho, C. T. (1996) Nonenzymatic deamidation of food proteins. *Crit. Rev. Food Sci. Nutr.* **36,** 225–255
61. Wright, H. T. (1991) Nonenzymatic deamidation of asparaginyl and glutaminyl residues in proteins. *Crit. Rev. Biochem. Mol. Biol.* **26,** 1–52
62. Tomita, S., and Shiraki, K. (2011) Why do solution additives suppress the heat-induced inactivation of proteins? Inhibition of chemical modifications. *Biotechnol. Prog.* **27,** 855–862
63. Privalov, P. L., and Gill, S. J. (1988) Stability of protein structure and hydrophobic interaction. *Adv. Protein Chem.* **39,** 191–234
64. Pettersen, E. F., Goddard, T. D., Huang, C. C., Couch, G. S., Greenblatt, D. M., Meng, E. C., and Ferrin, T. E. (2004) UCSF Chimera—a visualization system for exploratory research and analysis. *J. Comput. Chem.* **25,** 1605–1612

Heat-induced Irreversible Denaturation of the Camelid Single Domain VHH Antibody Is Governed by Chemical Modifications

Yoko Akazawa-Ogawa, Mizuki Takashima, Young-Ho Lee, Takahisa Ikegami, Yuji Goto, Koichi Uegaki and Yoshihisa Hagihara

J. Biol. Chem. 2014, 289:15666-15679.
doi: 10.1074/jbc.M113.534222 originally published online April 16, 2014
